ADVANCED MATERIALS

DOI: 10.1002/adma.200600375

Redox-Active Polypyrrole: Toward Polymer-Based Batteries**

By *Hyun-Kon Song* and *G. Tayhas R. Palmore**

One of the most important challenges in energy research is the development of an energy-storage device that can deliver electricity for longer periods of time at higher power demand.[1] A governing principle, as illustrated in Ragone plots of energy density (ED) versus power density (PD), is that the deliverable energy stored in a device decreases with an increasing demand for power or current.[2] At high power demands, the inefficiency of a device (i.e., loss of energy) is due to limitations involving the mass transfer of ions or sluggish reaction kinetics, or ionic or electric resistance involved within materials or at interfaces between different phases or materials.

Batteries and electric double-layer capacitors (EDLCs) are both ends of a wide spectrum of devices used to deliver power. Batteries are based on faradaic reactions (e.g., electrochemical reduction and oxidation); EDLCs are based on non-faradaic reactions (e.g., charging and discharging the electric double layer). Batteries are known for their high ED but low PD (ED = 20–100 W h kg^{-1} and PD = 50–200 W kg^{-1}), whereas ultracapacitors are the opposite (ED = 1–10 W h kg^{-1} and PD = 1000–2000 W kg^{-1}). The faradaic reactions on which batteries are based enable high EDs but charge-transfer reactions (e.g., from Li^+ to $LiCoO_x$) that accompany a phase change (e.g., from ions in electrolyte to solid) are kinetically slow processes, making batteries inappropriate for applications that require high PDs.[2] In contrast, the non-faradaic processes (i.e., charging) on which EDLCs are based involve the formation of an electric double layer at the interface between the electrolyte and the porous electrodes. This process is fast and facile, making EDLCs ideal for applications that require high PDs.

We describe herein a device for storing energy, the performance parameters of which reside between a rechargeable battery and an ultracapacitor. This system consists of two electrodes coated with polypyrrole (pPy) doped with different redox-active compounds: indigo carmine (IC) or 2,2′-azinobis(3-ethylbenzothiazoline-6-sulfonate) (ABTS) (Fig. 1). The resulting redox-active conducting polymers (pPy[IC] and pPy[ABTS]) form the basis of a battery that depends on the faradaic reactions of the redox-active dopants. This feature is uniquely different from batteries[3,4] or electrochemical capacitors[5] that depend solely on redox reactions or doping/dedoping of conducting polymers. The battery consisting of pPy[IC] | pPy[ABTS] shows significant enhancement in performance at high PDs (e.g., ED = 8 W h kg^{-1} at PD = 10^2 to 10^4 W kg^{-1}). This enhanced performance derives from a combination of merits found in batteries and EDLCs. The principle of energy storage is based on faradaic processes of redox-active dopants (battery-like) but the electrochemical reactions are surface confined without diffusion of the electroactive materials. Instead, the counterions in the electrolyte neutralize the charge on the electrode (EDLC-like). The porous structure of the conducting polymer provides an electrode with high surface area and enables counterions to access the redox-active dopants. In addition, the polymer matrix provides an environment that is conductive, leading to enhanced electron transfer between the base electrodes and the electroactive dopants.

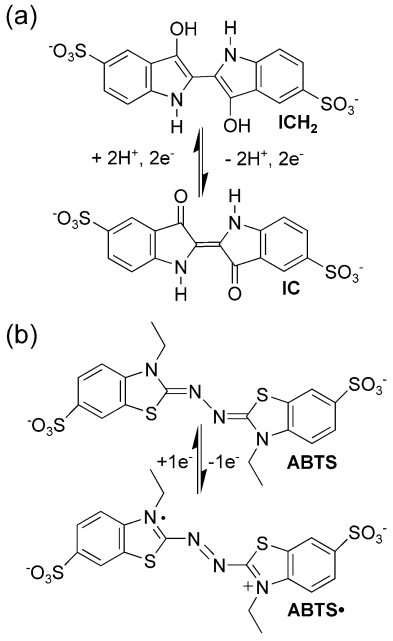

Figure 1. Molecular structures of oxidized and reduced forms of a) IC and b) ABTS.

The cationic charge that develops in pPy during the electropolymerization of pyrrole requires an influx of anions from the electrolyte to maintain charge neutrality.[6] Because the

[*] Prof. G. T. R. Palmore, Dr. H.-K. Song
Division of Engineering, Brown University
Providence, RI 02912 (USA)
E-mail: Tayhas_Palmore@brown.edu
Prof. G. T. R. Palmore
Department of Molecular Pharmacology, Physiology, and Biotechnology, Brown University
Providence, RI 02912 (USA)

[**] We thank the National Science Foundation for generous support. Supporting Information is available online from Wiley InterScience or from the author.

InterScience®
© 2006 WILEY-VCH Verlag GmbH & Co. KGaA, Weinheim

structures of each dopant (IC or ABTS, Fig. 1) include two sulfonate substituents, these compounds are anionic in both their oxidized and reduced forms. In addition, both IC and ABTS exhibit reversible redox chemistry at 52 and 570 mV (all potentials are reported vs. Ag/AgCl in this work), respectively, in a supporting electrolyte of 0.2 M HCl, pH 1. As such, these two characteristics, anionic character and reversible redox chemistry, make both compounds attractive choices for doping the conductive form of pPy.

PPy (pPy[dopant]) was electrodeposited onto a glassy carbon electrode from an aqueous solution of pyrrole and dopant (either IC or ABTS) by sweeping the potential cyclically. During electrodeposition, the current increased with each cycle, indicating the formation of conductive films of pPy doped with either IC or ABTS. Dark-blue films were electrodeposited regardless of dopant. Based on elemental analysis, the ratio of pyrrole subunits to IC or ABTS dopants in pPy[dopant] was estimated to be 10:1, giving one positive charge for every five subunits of pyrrole.[7]

Figure 2a shows the cyclic voltammograms (CVs) of the resulting films (pPy[IC] and pPy[ABTS]). Both polymers exhibit reversible redox behavior at potentials identical to their respective dopants in solution, indicating that the incorporation of IC or ABTS into pPy does not affect the redox potentials of the dopants. In addition, the CVs of both pPy[IC] and

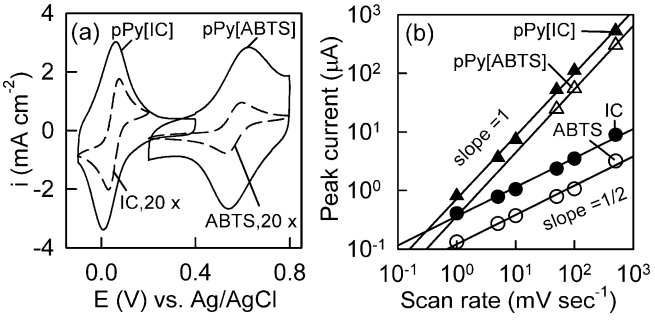

Figure 2. a) CVs (100 mV s^{-1}) and b) scan-rate dependence of peak currents of pPy[IC], pPy[ABTS], 0.25 mM IC, and 0.25 mM ABTS in 0.2 M HCl at pH 1. Glassy carbon (0.03 cm^2) was the working electrode used for all measurements.

pPy[ABTS] exhibit large faradaic and non-faradaic currents compared to the CVs of IC and ABTS in solution. The non-faradaic current of the pPy films is due to capacitive charging of the porous pPy film with high surface area. The large faradaic current of the pPy films is a result of high concentrations of IC or ABTS in the films (C_{film} in Table 1) that are confined to the surface of the electrode. Based on our calculations for a film with a thickness of 0.1 μm, both IC and ABTS appear to be highly concentrated in the pPy films compared to their solubility in water (i.e., $C_{film} \gg C_{max}$, solubility). As shown in Table 1, the concentration of IC and ABTS in the pPy films is 30 times higher than their maximum concentration in water. Thus, doping pPy with IC or ABTS during electrosynthesis overcomes the solubility limit of IC and ABTS

Table 1. Electrochemical properties of a redox-active component dissolved in solution and doped into films of pPy. The concentration of ABTS or IC in solution was 0.25 mM and the concentration of the electrolyte was 0.2 M HCl at pH 1. A glassy carbon working electrode (0.03 cm^2) was used. The film thickness of pPy[IC] and pPy[ABTS] = 0.1 μm. Q_{CV} = the voltammetric capacity calculated from the CV shown in Figure 2 (1 nA h = 3.6 μC). Q_{Th} = theoretical specific capacity, $k°$ = the standard rate constant, C_{max} = the solubility of redox-active molecule in water, and C_{film} = the concentration of redox-active dopant in the pPy film.

	IC		ABTS	
	Solution	pPy[IC]	Solution	pPy[ABTS]
$k°$ [cm sec^{-1}] × 10^3	7.9	26	15	9.1
Q_{CV} [nA h] at 100 mV s^{-1}	0.86	31	0.71	42
Conc. [mM]	C_{max}<50	C_{film}=1500	C_{max}<100	C_{film}=2900
Q_{Th} [mA h g^{-1}]	115	47	49	22

and produces a conductive film that is able to pass large faradaic currents.

Whether a redox-active molecule is confined to the surface of the electrode or dissolved in solution can be determined unambiguously by measuring CVs at different scan rates (Fig. 2b).[8–10] As expected, the peak currents in the CVs of both pPy[IC] and pPy[ABTS] are proportional to the scan rate, indicating that the redox-active molecule is confined to the surface of the electrode. In contrast, the peak currents of IC or ABTS in solution are proportional to the scan rate multiplied by 0.5, indicating that the redox-active molecule must diffuse to the electrode to exchange reducing equivalents.

Also shown in Table 1 are the rate constants for heterogeneous electron transfer ($k°$) for these films as calculated by the method of Nicholson.[11] Both films show values for $k°$ that are of the same order of magnitude as the redox-active dopants in solution. Because $k°$ is a measure of the ease by which a molecule relinquishes an electron, comparable values of $k°$ indicate that the molecule undergoes similar changes to its molecular structure regardless of whether it is a dopant in pPy or dissolved in solution.

The difference between the surface-confined and diffusion-controlled redox reactions also appears in their discharge curves. Shown in Figure 3 are discharge curves of each system at three different current densities (i.e., curves labeled *i*, *ii*, and *iii*). The maximum capacity at 0.3 V (nA h in abscissa) for both pPy[ABTS] and pPy[IC] (Fig. 3a and b) is much higher than that of ABTS or IC in solution (Fig. 3c and d) for all discharge currents. Moreover, compared to ABTS or IC in solution, the maximum capacity at 0.3 V for both pPy[ABTS] and pPy[IC] decreases less rapidly with increasing current density from *i* to *iii*. For example, the ratio of capacity at 0.3 V of curve *iii* to curve *i* is 72 % for pPy[ABTS] and 83 % for pPy[IC], whereas it is 15 % and 8.8 % for ABTS and IC in solution, respectively. The significance of a higher ratio of capacity at different discharge currents is that the surface-confined redox molecules in pPy[ABTS] and pPy[IC] are used more efficiently than ABTS and IC in solution, thereby overcoming the limit of mass transfer on the rate of power delivery.

 © 2006 WILEY-VCH Verlag GmbH & Co. KGaA, Weinheim

ADVANCED MATERIALS

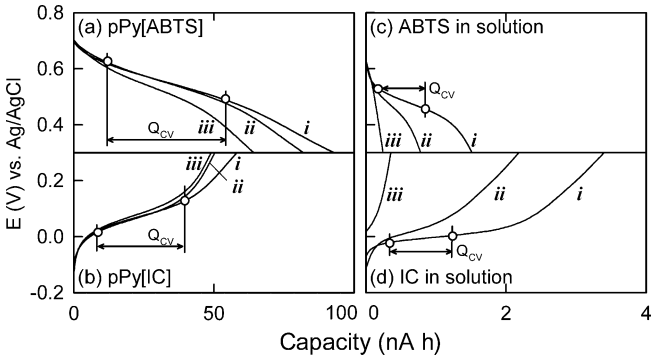

Figure 3. Discharge curves (i.e., chronopotentiograms) in 0.2 M HCl of a) pPy[ABTS], b) pPy[IC], c) 0.25 mM ABTS, and d) 0.25 mM IC. Current densities used were $i = 20$, $ii = 100$, and $iii = 1000$ μA cm^{-2}. Q_{CV} obtained at 100 mV s^{-1} (see Table 1) is indicated for each material. Experimental conditions were identical to those described in Figure 2.

Additionally, the superior efficiency of the surface-confined systems relative to the solution systems is confirmed by the dependency of Q_{CV} on scan rate (the amount of faradaic charge as measured by cyclic voltammetry). The value of Q_{CV} for pPy[ABTS] or pPy[IC] does not change significantly at scan rates ranging from 1 to 500 mV s^{-1} (see Supporting Information). Consequently, the value of Q_{CV} for pPy[ABTS] and pPy[IC] obtained at any scan rate below 500 mV s^{-1} corresponds to the size of the plateau region in discharge curve *i* (Fig. 3a and b). The plateau region in a discharge curve represents the amount of capacity derived from faradaic reactions. In contrast, Q_{CV} of the corresponding redox molecules in solution is highly dependent on the scan rate, decreasing with increasing scan rate from 1 to 500 mV s^{-1}. Thus, the value of Q_{CV} for ABTS and IC in solution obtained at 100 mV s^{-1} is smaller than the size of the plateau region in the corresponding discharge curve *i* (Fig. 3c and d). To obtain a value for Q_{CV} that is equal to the size of the plateau region in discharge curve *i* requires a scan rate of 10 mV s^{-1}.

Based on our findings described above, a rechargeable battery can be fabricated with pPy[IC] and pPy[ABTS] because these materials possess properties that are important to battery technology. First, both pPy[IC] and pPy[ABTS] exhibit reversible redox behavior at different potentials. Second, the concentrations of IC and ABTS in pPy[IC] and pPy[ABTS] are high, allowing for high faradaic currents. Third, concentration overpotentials associated with a mass-transfer limited reaction are circumvented by confinement of the redox-active molecules to the surface of the electrode. Thus, the rate of electron transfer between the electrode and IC in pPy[IC] or ABTS in pPy[ABTS] is fast compared to IC or ABTS in solution. The first property is required for a rechargeable battery and the second property affords a battery with high ED. The third property guarantees a battery with good performance characteristics at fast discharge rates. Based on the values of each electrode (Table 1), the theoretical capacity of a battery consisting of an anode of pPy[IC] and a cathode of pPy[ABTS] is estimated to be 54 C g^{-1} or 15 mA h g^{-1}. Thus, the theoretical capacity of this battery is one seventh the capacity of a lithium-ion battery composed of a lithiated graphite (LiC_6) anode and a $LiMn_2O_4$ cathode (ca. 100 mA h g^{-1}).

Figure 4a shows a diagram that illustrates electron and ion flow in a battery using pPy[IC] as the anode and pPy[ABTS] as the cathode. During charging, the IC in pPy[IC] is reduced at 52 mV with concurrent influx of protons from the electrolyte. Simultaneously, the ABTS in pPy[ABTS] is oxidized to the radical cation at 570 mV with concurrent influx of chloride anions from the electrolyte to maintain charge neutrality. During discharge the reverse reactions proceed at each electrode.

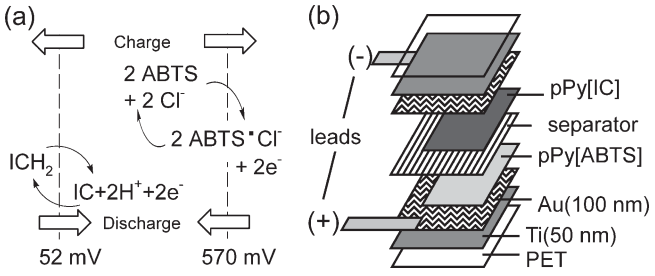

Figure 4. a) Electron and ion flow and b) expanded view of a battery based on a pPy[IC] anode and pPy[ABTS] cathode. PET: poly(ethylene terephthalate).

A rechargeable battery consisting of pPy[IC] as the anode and pPy[ABTS] as the cathode (pPy[IC] | pPy[ABTS]) was fabricated as shown in Figure 4b. Discharge curves from the resulting battery are shown in Figure 5a. Initially, the potential of pPy[ABTS] versus pPy[IC] decreases rapidly for all curves of *i* to *iv* due to capacitive discharging. The abrupt potential drop due to resistance or IR drop is observed only for the fastest discharge (*iv*). Subsequently, the decrease in poten-

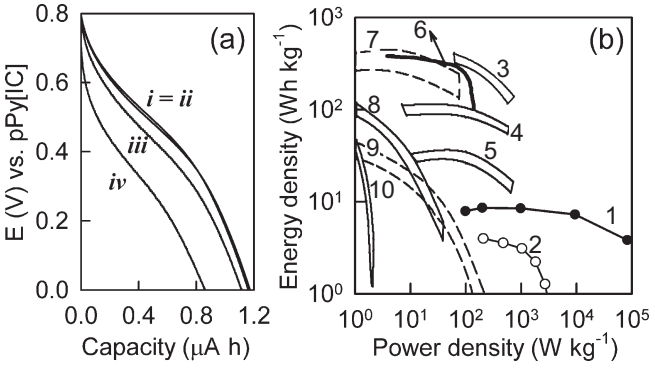

Figure 5. a) Discharge curves of a pPy[IC] | pPy[ABTS] battery (apparent area of each active electrode = 1 cm^2) obtained at various rates of discharge: $i = 10$, $ii = 10^2$, $iii = 10^3$, and $iv = 10^4$ μA cm^{-2}. b) Ragone plot for energy-storage devices [1,2]: 1, pPy[IC] | pPy[ABTS] battery; 2, an electric double layer capacitor (1800 F, 2.5 V, BCAP0008, Boostcap, Montena components, specified by the manufacturer); 3, high-temperature systems; 4, Ag–Zn; 5, Ni–Cd; 6, Li/MnO_2 (15 A h, Pouch cell, Bluestar, tested by Sandia National Lab.); 7, primary Li battery; 8, alkaline MnO_2; 9, lead–acid; 10, Leclanche.

© 2006 WILEY-VCH Verlag GmbH & Co. KGaA, Weinheim

tial becomes less rapid as ICH_2 in pPy[IC] is oxidized and $ABTS^{\bullet}$ in pPy[ABTS] is reduced. Finally, the potential decreases due to capacitive discharging at the same rate as shown in the initial period once all the energy stored in the electroactive species (IC and ABTS) is consumed. A significant decrease in capacity was not observed with increasing discharge currents up to 1 mA cm^{-2} (*i* to *iii*). This observation indicates that the pPy[IC] | pPy[ABTS] battery is most efficient (i.e., without energy loss) only when it is operated at PDs less than the value calculated from the discharge curve *iii* (e.g., 973 W kg^{-1} in Fig. 5b). For the curves *i* to *iii*, the specific capacity at which the potential reached 300 mV is estimated to be 15 mA h g^{-1}, which is the same value as for theoretical capacity.

Shown in Figure 5b is the ED of the pPy[IC] | pPy[ABTS] battery plotted as a function of PD (i.e., Ragone plots). Included in Figure 5b are data from other energy-storage devices for comparison. The ED was determined by integrating the discharge curves in Figure 5a between 300 and 800 mV. The average PD was obtained by dividing the ED by discharge time. Only the electroactive materials were included in the calculation of the mass of a pPy[IC] | pPy[ABTS] battery.

All curves in Figure 5b show a small decrease in ED at low PD (i.e., load) and an abrupt drop in ED above a critical PD. The most important feature of the pPy[IC] | pPy[ABTS] battery is that the decrease in ED is very small up to a critical PD of 10^4 W kg^{-1}. A value of 10^4 W kg^{-1} is significantly higher than the value of 10^3 W kg^{-1} reported for an EDLC (see 2 in Fig. 5b), a device commonly used for high-power applications. Moreover, the ED of the pPy[IC] | pPy[ABTS] battery (200 W kg^{-1}) is more than two times larger than that of the most advanced EDLC. An ED of 7.3 W h kg^{-1} at 10^4 W kg^{-1} is considered very high even when the mass of its casing is considered. For example, if a device based on pPy[IC] | pPy[ABTS] performs at just 10 % of the value shown in Figure 5b, the critical PD would decrease to 0.73 W h kg^{-1} at 10^4 W kg^{-1}, a value that is still much higher than that of electrochemical capacitors (6.4×10^{-4} W h kg^{-1} at 5700 W kg^{-1}). Thus, despite its low theoretical capacity when compared with a lithium-ion battery, the pPy[IC] | pPy[ABTS] battery is useful for high-power applications. At high rates of discharge, the pPy[IC] | pPy[ABTS] battery displays an ED that is higher than that of a lithium-ion battery.

Despite the unique features of the pPy[IC] | pPy[ABTS] battery, its capacity decreased with repeated charging and discharging, reaching 50 % of its initial capacity after 60 cycles at a discharge current of 10 μA cm^{-2}. Overoxidation of pPy at positive potentials (e.g., pPy[ABTS] at 0.7 V) is the main reason for this instability, based on the fact that the capacity of pPy[ABTS] decreased with each charge/discharge cycle, while the capacity of pPy[IC] remained unchanged. Overoxidation of pPy is known to reduce the conjugation in its chemical structure with an accompanying decrease in conductivity.[12] To overcome the instability of the cathode, conducting polymers that are more stable in an oxidative environment (e.g., poly-3,4-ethylenedioxythiophene)[4] currently are being tested as an alternative to pPy in the cathode. Nevertheless, we believe that the concept presented here, the molecular-level incorporation of electroactive molecules into conducting polymers, can provide a spectrum of materials useful for energy-storage devices.

Experimental

Half-Cell Experiments: For electrodeposition and other electrochemical measurements, a single-compartment cell was configured with three electrodes: a glassy carbon disk (working, 0.03 cm^2), a platinum gauze (counter), and an Ag/AgCl (reference, 0.197 V versus normal hydrogen electrode) connected to a potentiostat/galvanostat (EG&G, Model 273A). All potentials are reported versus Ag/AgCl. Pyrrole (200 mM) was electropolymerized in the presence of a 25 mM aqueous solution of either ABTS or IC. The voltage of the working electrode was cycled between 0.0 and 650 mV for 40 cycles at 100 mV s^{-1}. The thickness of the resulting films of pPy[ABTS] and pPy[IC] were measured with a surface profilometer (Dektak3, Veeco). All CVs and charge/discharge curves were performed in an aqueous electrolyte of 0.2 M HCl. The working electrode used to evaluate films of pPy[ABTS] and pPy[IC] was a glassy carbon electrode coated with these films. The working electrode used to evaluate ABTS and IC in solution was a clean glassy carbon electrode immersed in the electrolyte containing 0.25 mM ABTS or IC. Prior to discharge, films of pPy[ABTS] and pPy[IC] were charged at +700 mV or –100 mV, respectively. The time in the abscissa of the discharge curves (potential vs. time) was converted to capacity by: capacity = discharge current × time (Nicholson method). Rate constants for heterogeneous electron transfer (k°) were obtained from the difference in the potential of the anodic and cathodic peaks in CVs using the method of Nicholson [11]. Diffusion coefficients (D, 10^{-6} cm^2 s^{-1}) for IC ($D_{IC} = 6.0$) [8] and ABTS ($D_{ABTS} = 3.22$) [13] were used to calculate k° for IC and ABTS in solution, respectively. Diffusion coefficients [14] for a proton ($D_{H^+} = 93$) and a chloride ion ($D_{Cl^-} = 20$) were used to calculate k° for pPy[IC] and pPy[ABTS], respectively, because IC and ABTS do not diffuse out of pPy during charging and discharging but instead are charge compensated by the movement of protons and chloride ions.

Surface Concentration: The concentration of IC or ABTS in pPy (C_{film}) is calculated from: $C_{film} = Q_{CV}/(n F A d)$, where Q_{CV} is the voltammetric capacity, F is Faraday's constant (96500 C (mol e$^-$)$^{-1}$, A is the geometric area of the electrode (0.03 cm^2), and d is the thickness of the pPy film, as measured with a surface profilometer. Q_{CV} was obtained by integrating the cathodic peak in CVs of IC and pPy[IC] and the anodic peak in CVs of ABTS and pPy[ABTS] at 100 mV s^{-1}.

Theoretical Specific Capacity (Q_{Th}): The value of Q_{Th} corresponding to pPy[IC] or pPy[ABTS] was calculated from: $Q_{Th} = n F/M_w$, where n is the moles of electrons corresponding to the reduction or oxidation of one mol of IC or ABTS, respectively and M_w is the molecular weight of a repeat unit of pPy[IC] (1137.2 g mol^{-1}) or pPy[ABTS] (1219.6 g mol^{-1}). The repeat unit was taken to be a decamer of pyrrole units with a corresponding IC or ABTS unit based on the 10:1 ratio of pyrrole to IC or ABTS in these films [7].

Battery Experiments: Gold/titanium/poly(ethylene terephthalate) (Au/Ti/PET) flags were used as flexible electrodes. These electrodes were fabricated by coating a PET substrate first with an adhesion layer of Ti (50 nm) followed by a layer of Au (100 nm) using an electron-beam evaporator. The geometric area of the electrodes exposed to electrolytes during electrodeposition was 1 cm^2, which was achieved by blocking the remaining electroactive surface with Kapton tape. Both pPy[IC] and pPy[ABTS] were electrodeposited onto the surface of the Au/Ti/PET substrates using the same procedure as described above. A glass-fiber filter (Whatman, GF/C) was used as a separator between the two electrodes coated with doped pPy. The entire assembly was encapsulated with Kapton tape except the two leads from both electrodes and a portion of the separator. The electrolyte

 © 2006 WILEY-VCH Verlag GmbH & Co. KGaA, Weinheim

ADVANCED MATERIALS

was 0.2 M HCl, which was injected into the battery cell through the exposed portion of the separator. The battery was fully charged by applying +800 mV on pPy[ABTS] versus pPy[IC], and subsequently discharged at a constant current. To calculate the specific capacity, the amount of redox-active pPy (m) in each sample was determined by dividing the voltammetric capacity Q_{CV} by the theoretical specific capacity Q_{Th}. The value for Q_{CV} was obtained from the CV of each electrode (see Supporting Information) as described in the Surface Concentration section above. The value for Q_{Th} is given in Table 1. Thus, $m = 19$ μg for pPy[IC]/Au/Ti/PET based on the value of $Q_{CV} = 870$ nA h, and $m = 35$ μg for pPy[ABTS]/Au/Ti/PET based on the value of $Q_{CV} = 760$ nA h (see Supporting Information, Table 1).

Received: February 23, 2006
Final version: April 11, 2006
Published online: June 8, 2006

[1] D. Linden, T. B. Reddy, *Handbook of Batteries*, McGraw-Hill, Seoul **2001**.
[2] B. E. Conway, *Electrochemical Supercapacitors*: *Scientific Fundamentals and Technological Applications*, Kluwer Academic/Plenum, New York **1999**.
[3] D. Naegele, R. Bittihn, *Solid State Ionics* **1988**, *28*, 983.
[4] P. Novak, K. Muller, K. S. V. Santhanam, O. Haas, *Chem. Rev.* **1997**, *97*, 207.
[5] C. Arbizzani, M. Mastragostino, L. Meneghello, *Electrochim. Acta* **1996**, *41*, 21.
[6] N. C. Billingham, P. D. Calvert, in *Advances in Polymer Science*, Vol. 90 (Eds: H. Benoit, H. Cantow), Springer, New York **1989**, p. 1.
[7] H. K. Song, G. T. R. Palmore, *J. Phys. Chem. B* **2005**, *109*, 19278.
[8] T. Komura, T. Kobayasi, T. Yamaguti, K. Takahasi, *J. Electroanal. Chem.* **1998**, *454*, 145.
[9] A. J. Bard, L. R. Faulkner, *Electrochemical Methods*: *Fundamentals and Applications*, Wiley, New York **1980**.
[10] G. T. R. Palmore, D. K. Smith, M. S. Wrighton, *J. Phys. Chem. B* **1997**, *101*, 2437.
[11] R. S. Nicholson, *Anal. Chem.* **1965**, *37*, 1351.
[12] J. Rodriguez, H.-J. Grande, T. F. Otero, in *Handbook of Organic Conductive Molecules and Polymers*, Vol. 2 (Ed: H. S. Nalwa), Wiley, New York **1997**, p. 415.
[13] G. T. R. Palmore, H. H. Kim, *J. Electroanal. Chem.* **1999**, *464*, 110.
[14] P. Vanysek, in *CRC Handbook of Chemistry and Physics* (Ed: D. R. Lide), 74th ed., CRC Press, Boca Raton, FL **1993**, p. 5.

 © 2006 WILEY-VCH Verlag GmbH & Co. KGaA, Weinheim